2012

Carbon nanotube nanoweb-bioelectrode for highly selective dopamine sensing

Jie Zhao
University Of Wollongong, jz544@uow.edu.au

Weimin Zhang
University Of Wollongong, weimin@uow.edu.au

Peter Sherrell
University of Wollongong, psherrel@uow.edu.au

Joselito M. Razal
University of Wollongong, jrazal@uow.edu.au

Xu-Feng Huang
University of Wollongong, xhuang@uow.edu.au

See next page for additional authors

ACS APPLIED MATERIALS & INTERFACES

Letter

www.acsami.org

Carbon Nanotube Nanoweb–Bioelectrode for Highly Selective Dopamine Sensing

Jie Zhao,[†] Weimin Zhang,[†,‡] Peter Sherrell,[†] Joselito M. Razal,[†] Xu-Feng Huang,[§] Andrew I. Minett,[‡] and Jun Chen*[,†]

[†]Intelligent Polymer Research Institute, ARC Centre of Excellence for Electromaterials Science, Australian Institute of Innovative Materials, Innovation Campus, and [§]Centre for Translational Neuroscience, IHMRI, School of Health Sciences, University of Wollongong, NSW 2522, Australia

[‡]Laboratory for Sustainable Technology, School of Chemical and Biomolecular Engineering, University of Sydney, Sydney, NSW 2006, Australia

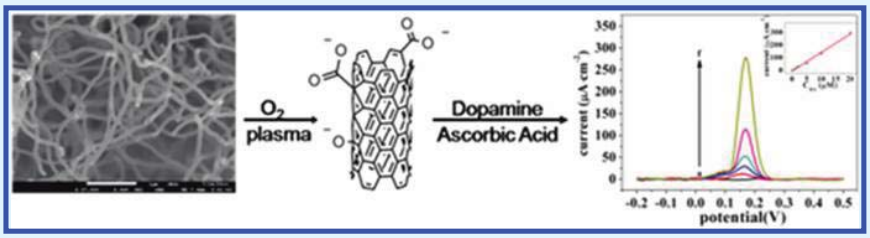

ABSTRACT: A highly sensitive and selective dopamine sensor was fabricated with the unique 3D carbon nanotube nanoweb (CNT-N) electrode. The as-synthesised CNT-N was modified by oxygen plasma to graft functional groups in order to increase selective electroactive sites at the CNT sidewalls. This electrode was characterized physically and electrochemically using HRSEM, Raman, FT-IR, and cyclic voltammetry (CV). Our investigations indicated that the O_2-plasma treated CNT-N electrode could serve as a highly sensitive biosensor for the selective sensing of dopamine (DA, 1 μM to 20 μM) in the presence of ascorbic acid (AA, 1000 μM).

KEYWORDS: *dopamine, ascorbic acid, carbon nanotube nanoweb, O_2 plasma, biosensor*

1. INTRODUCTION

Dopamine (DA) is one of most important neurotransmitters across all animals, including humans. Alterations in DA contribute to the development of a number of severe mental illnesses, such as Parkinson's disease, Schizophrenia and depression.[1−3] Clearly, an early detection of DA is important; therefore, detection of DA using voltametric methods has been widely reported,[4] because electrochemical measurements require simple equipment and produce fast detection. However, a critical issue that needs to be overcome is the selectivity of the electrode due to the overlapping oxidation potential (E_{ox}) of DA with other chemicals present in the central nervous system. In particular, ascorbic acid (AA) has been the major interfering species due to its abundance in serum samples (much higher than DA) and having a close E_{ox} to that of DA.[5] In order to selectively detect DA, novel electrode materials including polymer-based films[6−9] and metal nanoparticles have been developed; however, there are still barriers that need to be overcome, such as inference from AA and low DA oxidation signals.[10−12] Recently, carbon nanomaterials[13−18] are proving to be among the outstanding candidates as novel platforms for sensing because their bio-electrocatalytic properties, chemical functionalities, and physical stability can be quite easily tailored. Among the carbon nanomaterials, carbon nanotube (CNT) has been particularly attractive as novel platform for DA sensing. Recent studies showed that the utilization of CNT-based electrodes is conducive to obtain a significant separation of E_{ox} for both DA and AA, which could improve the selective sensing of DA against up to 200 μM AA with improved sensitivity (increased voltametric current signals).[19] These merits are perhaps attributed to the highly electroractive surface area and the fast electron-transfer properties of CNT-based electrodes.[20] However, up to now, most CNT-based electrodes have been utilizing randomly structured CNT materials, which exhibit poor electric contact with current collector of the electrode and also low utilization efficiency of the CNT materials. Therefore in this study, we report a highly efficient 3D carbon nanoweb electrode[21] as a novel platform for the selective detection of DA over AA. The as-synthesized CNT-N electrode consisting of a highly porous tangled CNT top network layer and a dense bottom CNT-carbon composite layer provides an ideal configuration for a highly sensitive (high surface area) and an electrically and mechanically robust electrode (i.e., the active CNT network is intimately connected with the highly conducting support).[22] Here, we demonstrate that after an oxygen (O_2) plasma treatment is employed, the CNT-N shows

Received: October 30, 2011
Accepted: December 7, 2011
Published: December 7, 2011

dx.doi.org/10.1021/am201508d | *ACS Appl. Mater. Interfaces* 2012, 4, 44–48

extremely promising results in the selective detection of DA in the presence of AA using differential pulse voltammetry (DPV).

2. EXPERIMENTAL SECTION

2.1. Reagents and Materials. Dopamine hydrochloride (DA) and ascorbic acid (AA) were obtained from Fluka and Sigma, respectively. Both DA and AA solutions were freshly prepared before electrochemical tests. A phosphate buffer saline (PBS) was prepared from NaH_2PO_4 (Fluka) and Na_2HPO_4 (Sigma-Aldrich). The pH value of the buffer solution was adjusted to 7.0 with NaOH (Chem-supply).

2.2. Electrode Preparation. The 3D CNT-N were synthesised by the modified chemical vapour deposition (CVD) method as described in our previous report.[21] The entangled carbon nanotube/conductive carbon networks (CNT-N) were synthesised by the decomposition of acetylene over Iron(III) Tosylate (Fe(III)pTs) thin films which were spin-coated onto quartz plate. First, a piece of Fe(III)pTs thin film coated quartz plate was placed in a chemical vapor deposition (CVD) furnace at 60°C in an argon atmosphere. Hydrogen was introduced at a flow rate of 20sccm to reduce the Fe^{3+} to catalytically active Fe^0 centres at 550°C. Followed with the decomposition of acetylene (with a gas flow of C_2H_2/H_2 at 15/5sccm) over the Fe^0 centers to induce the CNT growth at 800°C for 30 min. Finally, the furnace was cooled down to room temperature under an Argon atmosphere. After the growth, a free standing piece of NanoWeb was transferred from quartz plate to ITO-coated glass and ready for further investigations. The oxygen (O_2) plasma treatment for CNT-N electrode was performed using a plasma generator (Harrick Plasma, USA) at room temperature and 0.6 Torr O_2 pressure for 15 min.

2.3. Characterization. The HRSEM images of the electrode surface were taken in a JSM7500FA field emission scanning electron microscope (JEOL Ltd, Japan) to monitor the CNT-N morphology. Raman spectra were recorded using a Jobin-Yvon Horbia 800 (Horiba Ltd., France) with 632.8 nm HeNe laser excitation. The Fourier transform infra red (FT-IR) spectra of CNT-N were obtained with AIM-8800 automatic infrared microscope (Shimadzu Corporation, Japan). Both Raman and FT-IR were employed to determine and/or confirm the functional groups introduced by O_2 Plasma. The Cyclic voltammogram (CV) and the differential pulse voltammogram (DPV) were performed using a CHI720C electrochemical workstation (CH Instruments Inc., USA). The following parameters were used to record DPV. The amplitude was 0.05 V. The pulse width was 0.05 s. The sample width was 0.025 s, and the pulse period was 0.2 s. All measurements were conducted at room temperature in a standard three-electrode cell that consists of the CNT-N working electrode, a Pt mesh counter electrode, and an Ag/AgCl reference electrode.

3. RESULTS AND DISCUSSION

3.1. CNT-N. Figure 1A shows the digital image of a small piece of freestanding CNT-N (CNT-N) peeled off from quartz plate. The SEM image of the top surface of the CNT-N (Figure 1B) reveals an entangled CNT structure with a average of ~60 nm diameter. In addition, the insert TEM image also confirms a clear nanotube structure of the entangled CNTs. This top layer forms a highly porous entangled structure ideal for providing large surface area per unit volume electrodes. Followed with cross-section SEM images (Figure 1C, D), the cross-sectional

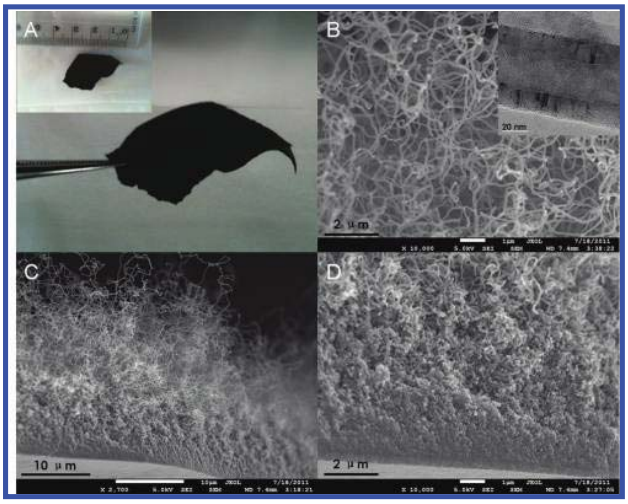

Figure 1. Physical characterisation of CNT-N: (A) digital image of free-standing CNT-N, (B) surface morphology of CNT-N and TEM image of as-synthesised CNT (the inset), and (C, D) SEM images of cross-sectional area CNT-N.

view of the CNT-N illustrates that part of the tangled porous CNT network is intimately connected to a dense carbon layer (bottom). This bottom layer forms a mechanically robust continuous support layer for the entangled CNT network and simultaneously provides lateral electrical connection with a low surface resistance of 70 Ω/□. Therefore, the CNT-N provides a unique 3D architecture that can be directly used as an electrode maintaining the original porous structure.[22]

3.2. Plasma Treatment for the Electrode. The as-synthesised CNT-N is hydrophobic and chemically inert which impedes electrochemical investigations in aqueous environments. From contact angle analysis, it presents a significantly high H_2O contact angle of 147.5° (Figure 2A inset, hydrophobic) for the original CNT-N. Surface treatment or functionalisation has been shown to be critical for the interaction between the CNTs surface and biomolecules.[23] Recent investigation indicated that cold gas plasma is an effective treatment for functionalisation of CNTs without detrimental effect on the original CNT structure,[24] whereas harsh chemical oxidation (using HNO_3, H_2SO_4, and $KMnO_4$) strongly etches CNT sidewalls and results in CNT shortening which negatively effects their electronic properties.[25,26] The CNT-N was treated with O_2 plasma in order to render the CNT surface with oxygen-containing functional groups. The FT-IR analysis (Figure 2A) confirmed different appended surface species between the as-synthesized and O_2 plasma-treated CNT-N. The as-synthesized CNT-N showed virtually no surface functionality while the plasma-treated CNT-N revealed signature vibration bands for hydroxyl at 914 and 1414 $cm^{-1}$and carboxyl and carbonyl at 1605 and 1722 cm^{-1}, respectively. In addition, the Raman spectra (Figure 2B) for CNT-N show clear differences in the spectral response after O_2 plasma treatment. The D band peak position is constant for both samples at approximately 1330 cm^{-1}, however after plasma treatment the G peak, at around 1580 cm^{-1} is split into two separate peaks. Previous reports have demonstrated that the higher wavenumber peak arises from defects along the CNT sidewall.[27−29] The increased I_D/I_G (from 1.19 to 1.24) also supports the generation of defect sites after plasma treatment, as suggested by the FT-IR spectra. Furthermore, the plasma

dx.doi.org/10.1021/am201508d | ACS Appl. Mater. Interfaces 2012, 4, 44−48

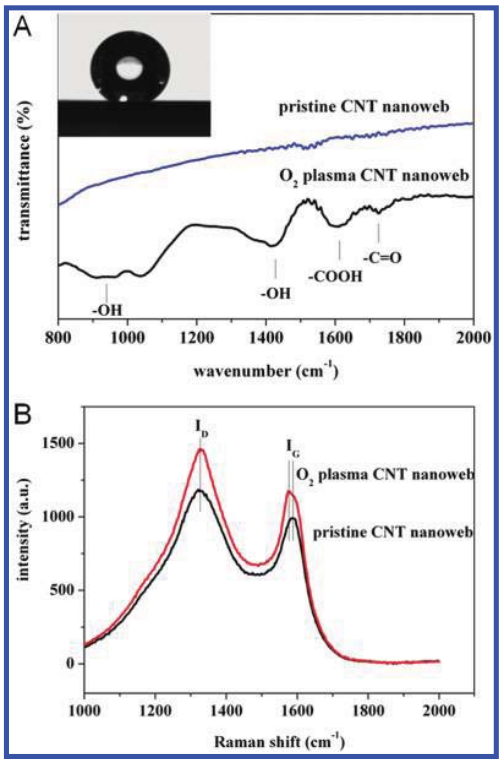

Figure 2. (A) FT-IR spectra and (B) Raman spectra of the pristine and O_2 plasma-treated CNT-N.

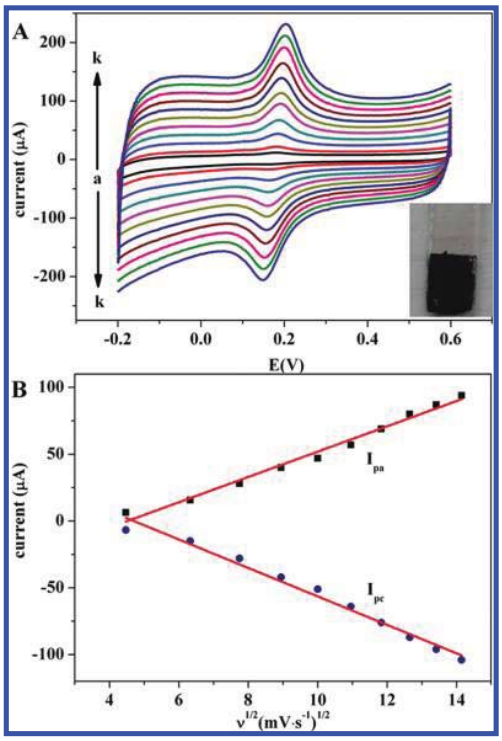

Figure 3. (A) CV of the O_2 plasma-treated CNT-N electrode in 20 μM DA solution (pH 7.0 PBS) at different scan rates (a–k): 20, 40, 60, 80, 100, 120, 140, 160, 180, and 200 mV s^{-1}; (B) calibration plots of peak current to square root of scan rates obtained from CV.

treatment resulted in significantly improved wettability under aqueous environments. In comparison, no H_2O contact angle is measurable (close to 0°, fully hydrophilic) after O_2 plasma treatment, compared with a contact angle of 147.5° before O_2 plasma treatment. This kind of improvement could play a important role in sensing performance.

3.3. Cyclic Voltammetry. Figure 3A shows the cyclic voltammograms (CVs) of a plasma treated CNT-N bioelectrode in PBS containing 20 μM DA. The CVs clearly show pairs of symmetric redox peaks that can be ascribed to the electron transfer-chemical reaction-electron transfer (ECE) mechanism. The first step of DA oxidation involves the two-electron transfer and generation of dopaminoquinone; dopaminoquinone then transforms to leucodopaminechrome, which is further oxidized to dopaminechrome in pH 7 solutions as follows:[30]

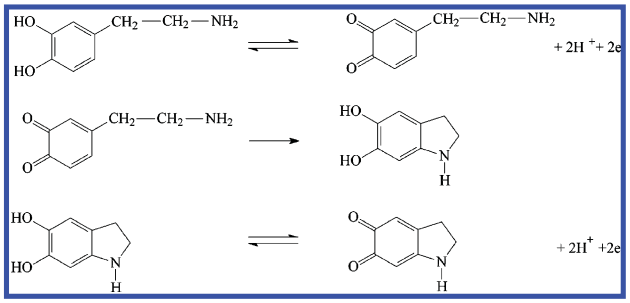

The anodic and cathodic peak current (I_{pa} and I_{pc}, respectivey) were shown to increase linearly with the square root of scan rate in the investigated range (from 20 to 200 mV s^{-1}) (Figure 3B). The linear relationship for anodic peak current response is represented by $I_{pa} = 9.47\nu^{1/2} - 42.03$ (R = 0.992), which suggests a diffusion-controlled oxidation process of DA is the dominant mechanism. These processes signified reversible electron transfer reactions that exhibited close to ideal and reversible kinetic behaviours at the CNT-N electrode.[31]

3.4. Differential Pulse Voltammogram Determination of DA and AA. The selective determination of DA in the presence of ascorbic acid (AA) was investigated using differential pulse voltammetry (DPV). Figure 4A shows the representative DPV curves of various DA concentrations in PBS solution (pH 7.0) with the presence of 1000 μM AA using plasma-treated CNT–N electrode. The peak currents (within 5% variable using diffent electrodes) assigned to the oxidation of DA (at 0.17 V *vs.* Ag/AgCl) show a linear response with increasing DA concentration represented by I_{pa} =14.69C_{DA} − 5.84 (R = 0.996) (Figure 4B), whereas no apparent DPV signal was observed for AA. For the comparison, when using a pristine CNT-N electrode under identical testing conditions (Figure 5A), it is noted that AA is detected at 0.09 V vs Ag/AgCl and an overlapping signal was observed when a mixture of DA and AA (at a DA/AA ratio of 0.02) was evaluated. Furthermore, the plasma treated CNT-N also showed significantly increased signal (i.e., I_{pa}) than that of pristine CNT-N, which may be due to the increased wettability. The I_{pa} for a 20 μM DA solution at a plasma treated CNT-N electrode (278 μA cm^{-2}) was 17 times higher than that of pristine electrode under identical testing conditions (16 μA cm^{-2}, Figure 5B). This result showed excellent combined selectivity and sensitivity relative to literature reports that utilized other electrodes, 2–70 μM for poly (vinyl alcohol),[32] 2–80 μM for poly-chromotrope,[33] 24–384 μM for pyrolytic graphite.[34] Better sensitivity of 0.2–45.8 μM was demonstrated for poly-Tiron film; however, the response of AA is much stronger than that of DA and the

dx.doi.org/10.1021/am201508d | ACS Appl. Mater. Interfaces 2012, 4, 44–48

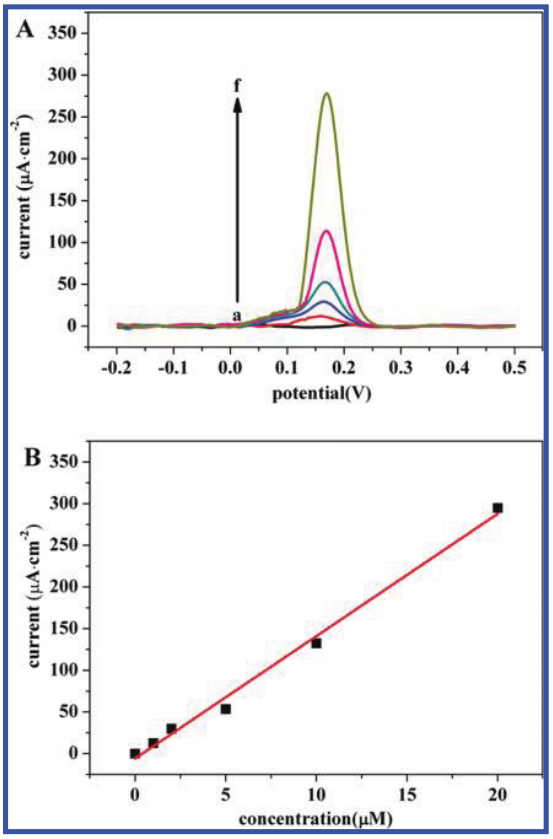

Figure 4. (A) DPV of different concentration DA (a) 0, (b) 1, (c) 2, (d) 5, (e) 10, and (f) 20 μM in the presence of 1000 μM AA on the O_2 plasma-treated CNT-N in pH 7.0 PBS. (B) Calibration plots of peak current (within 5% variable using diffent electrodes) to the concentration of DA from DPV on the O_2 plasma-treated CNT-N.

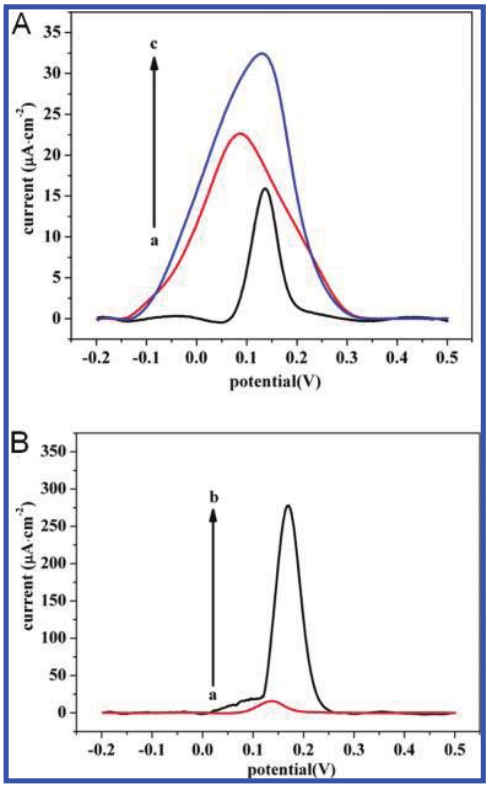

Figure 5. (A) DPV of (a) 20 μM DA, (b) 1000 μM AA, and (c) 20 μM DA and 1000 μM AA on the pristine CNT-N in pH 7.0 PBS. (B) DPV of (a) 20 μM DA on the pristine CNT-N and (b) 20 μM DA and 1000 μM AA on the O_2 plasma-treated CNT-N in pH 7.0 PBS.

correlation coefficient (0.991) is much lower than that in our study.[35]

The above demonstrated selective detection of plasma-treated CNT-N electrode towards DA at DA/AA concentration ratio (from 1:1000 to 20:1000) may be ascribed to electrostatic interactions. At solution of pH 7.0, the CNT surface functional groups are predominantly deprotonated, whereas DA and AA are dissociated, hence an electrostatic attraction of cationic DA to the surface of nanoweb is preferred over the anionic AA to which electrostatic repulsion is expected to occur. The high sensitivity may be due to the combination of several positive attributes of the plasma treated CNT-N. The three-dimensional and highly conductive network provides a large specific surface area that improves both the ionic and electronic transport capacities.[36] By rendering the CNT surface more hydrophilic, the interaction with polar molecules is significantly enhanced. This effect is best displayed by the increased I_{pa} suggesting that higher amounts of DA penetrate into the 3D nanoweb architecture due to the increased hydrophilicity after plasma treatment. In addition, the $\pi-\pi$ interactions between CNTs and DA that is absent for AA could be another contributing factor.[37]

4. CONCLUSIONS

The O_2 plasma-treated CNT-N electrode shows an excellent selectivity and sensitivity in detecting DA in the presence of AA. It showed a mass diffusion control process and significantly reversible electron transfer reactions in the dopamine detection. By using DPV method, the linear of anodic current peaks of DA was covered from 1 μM to 20 μM. In spite of the coexistence of AA, there was just a single oxidation curve, corresponding to DA, and no inference towards the peak current of DA. Promised increased selectivity was demonstrated in this study using plasma-treated CNT-N as the electrode, showing insignificant interferences in the presence of AA. Briefly the O_2-plasma treated CNT-N electrode has the potential to be used and developed into a truly selective dopamine sensor, whereas the response from AA is negligible.

AUTHOR INFORMATION

Corresponding Author

*E-mail: junc@uow.edu.au.

ACKNOWLEDGMENTS

The authors are grateful for the financial support of this work by the Australian Research Council Discovery Grant (ARC DP0877348).

REFERENCES

(1) Conway, K. A. *Science* **2001**, *294*, 1346−1349.
(2) Bird, E. D.; Spokes, E. G.; Iversen, L. L. *Science* **1979**, *204*, 93−94.
(3) Rubi, B.; Maechler, P. *Endocrinology* **2010**, *151*, 5570−5581.
(4) Ali, S. R.; Parajuli, R. R.; Balogun, Y.; Ma, Y.; He, H. *Sensors* **2008**, *8*, 8423−8452.
(5) Hou, S.; Kasner, M. L.; Su, S.; Patel, K.; Cuellari, R. *J. Phys. Chem. C* **2010**, *114*, 14915−14921.

(6) Ensafi, A. A.; Taei, M.; Khayamian, T.; Arabzadeh, A. *Sens. Actuators, B Chem.* **2010**, *147*, 213−221.
(7) Erdogdu, G.; Mark, H. B.; Karagozler, A. E. *Anal. Lett.* **1996**, *29*, 221−231.
(8) Xu, H. T.; Kitamura, F.; Ohsaka, T.; Tokuda, K. *Anal. Sci.* **1994**, *10*, 399−404.
(9) Lin, X.; Zhang, Y.; Chen, W.; Wu, P. *Sens. Actuators, B* **2007**, *122*, 309−314.
(10) Huang, J.; Liu, Y.; Hou, H.; You, T. *Biosens. Bioelectron.* **2008**, *24*, 632−637.
(11) Raj, C. R.; Okajima, T.; Ohsaka, T. *J. Electroanal. Chem.* **2003**, *543*, 127−133.
(12) Tian, Z. Q.; Jiang, S. P.; Liu, Z. C.; Li, L. *Electrochem. Commun.* **2007**, *9*, 1613−1618.
(13) Cao, X. H.; Zhang, L. X.; Cai, W. P.; Li, Y. Q. *Electrochem. Commun.* **2010**, *12*, 540−543.
(14) Babaei, A.; Babazadeh, M.; Momeni, H. *Int. J. Electrochem. Sci.* **2011**, *6*, 1382−1395.
(15) Jia, N.; Wang, Z.Y.; Yang, G.F.; Shen, H.B.; Zhu, L.Z. *Electrochem. Commun.* **2007**, *9*, 233−238.
(16) Tan, L.; Zhou, K. G.; Zhang, Y. H.; Wang, H. X.; Wang, X. D.; Guo, Y. F.; Zhang, H. L. *Electrochem. Commun.* **2010**, *12*, 557−560.
(17) Xu, L. Q.; Yang, W. J.; Neoh, K. G.; Kang, E. T.; Fu, G. D. *Macromolecules* **2010**, *43*, 8836−8839.
(18) Zhang, L.; Geng, W. C.; Qiao, S. Z.; Zheng, H. J.; Lu, G. Q.; Yan, Z. F. *ACS Appl. Mater. Interfaces* **2010**, *2*, 2767−2772.
(19) Viry, L.; Derre, A.; Poulin, P.; Kuhn, A. *Phys. Chem. Chem. Phys.* **2010**, *12*, 9993−9995.
(20) Cui, H.; Cui, Y.; Sun, Y.; Zhang, K.; Zhang, W. *Nanotechnology* **2010**, *21*, 215601−215608.
(21) Chen, J.; Minett, A. I.; Liu, Y.; Lynam, C.; Sherrell, P.; Wang, C. *Adv. Mater.* **2008**, *20*, 566−570.
(22) Frackowiak, E.; Metenier, K.; Bertagna, V.; Beguin, F. *Appl. Phys. Lett.* **2000**, *77*, 2421−2423.
(23) Shim, M.; Kam, N. W. S.; Chen, R. J.; Li, Y.; Dai, H. *Nano Lett.* **2002**, *2*, 285−288.
(24) Li, W.; Bai, Y.; Zhang, Y. K.; Sun, M. L.; Cheng, R. M.; Xu, X. C.; Chen, Y.; Mo, Y. *Synth. Met.* **2005**, *155*, 509−515.
(25) Zhang, X.; Lei, L.; Xia, B.; Zhang, Y.; Fu, J. *Electrochimica Acta.* **2009**, *54*, 2810−2817.
(26) Zhang, J.; Zou, H.; Qing, Q.; Yang, Y.; Li, Q.; Liu, Z.; Guo, X.; Du, Z. *J. Phys. Chem. B* **2003**, *107*, 3712−3718.
(27) Lin, W.; Moon, K. S.; Zhang, S.; Ding, Y.; Shang, J.; Chen, M.; Wong, C. *ACS Nano* **2010**, *4*, 1716−1722.
(28) Delosarcos, T.; Gunnargarnier, M.; Oelhafen, P.; Mathys, D.; Wonseo, J.; Domingo, C.; Vicentegarciaramos, J.; Sanchezcortes, S. *Carbon* **2004**, *42*, 187−190.
(29) Curran, S. A.; Talla, J. A.; Zhang, D.; Carroll, D. L. *J. Mater. Res.* **2011**, *20*, 3368−3373.
(30) Luczak, T. *Electroanalysis* **2008**, *20*, 1639−1646.
(31) Chen, T. *Experimental Electrochemistry*; Xiamen University Press: Xiamen, China, 1993.
(32) Li, Y.; Lin, X. *Sens. Actuators, B* **2006**, *115*, 134−139.
(33) Lin, X.; Zahuang, Q.; Chen, J.; Zhang, S.; Zheng, Y. *Sens. Actuators, B* **2007**, *125*, 240−245.
(34) Silva, R. P. D; Lima, A. W. O.; Serano, S. H. P. *Anal. Chim. Acta* **2008**, *612*, 89−98.
(35) Ensafi, A. A.; Taei, M.; Khayamian, T. *Int. J. Electrochem. Sci.* **2010**, *5*, 116−130.
(36) Zhang, M.; Gorski, W. *J. Am. Chem. Soc.* **2005**, *127*, 2058−2059.
(37) Snejdarkova, M.; Poturnayova, A.; Rybar, P.; Lhotak, P.; Himl, M.; Flidrova, K.; Hianik, T. *Bioelectrochemistry* **2010**, *80*, 55−61.